RSC Advances

PAPER

View Article Online
View Journal | View Issue

Open Access Article. Published on 19 November 2019. Downloaded on 12/9/2025 3:22:16 AM.
This article is licensed under a Creative Commons Attribution-NonCommercial 3.0 Unported Licence.

Check for updates

Cite this: *RSC Adv.*, 2019, **9**, 37562

Advanced catalytic oxidation process based on a Ti-permanganate (Mn/Ti-H^+) reaction for the treatment of dye wastewater

Rafia Azmat,* Anum Khursheed, Ailyan Saleem and Noshab Qamer

This article discusses the titanium (Ti)-based permanganate advanced catalytic oxidation process (ACOP) for the possible recovery of thousands of tons of dye wastewater. The heterogeneous catalyst TiO_2 in the solid state employed in the liquid phase reaction mixture with dye and potassium permanganate was recovered and reused several times for reproducible results. The kinetics were examined at various operational parameters like the effect of dyes, the effect of oxidants, the amount of catalysts, and the effect of acids, temperature, and various organic and inorganic additives used in the textile industry. The kinetics of advanced oxidation and the mechanism of dye de-coloration and degradation were monitored using the Congo red (CR) dye as a model in an aqueous medium and then applied to other dyes and real dye wastewater samples. The color removal was up to 98%, with the removal efficiency being linear with the dose at a particular time. This method could exhibit the complete color removal of the dye wastewater, leading to mineralization coupled with a change in the oxidation state of Mn from +7 to +2. The method also improved the BOD/COD ratio, followed by an increase in the salinity of the recycled water. This indicated that this method can be used not only for the highly efficient de-colorization of dye wastewater but also as a preliminary step for the utilization of the dye wastewater after its recycling. The newly developed system was proven to be very cost-effective and eco-friendly with low sludge quantity, which contained numerous nitrogenous compounds, and this was validated by FTIR and HPLC analyses; thus, the system may be used in treatment plants for the recovery of wastewater.

Received 24th April 2019
Accepted 5th October 2019

DOI: 10.1039/c9ra03045j

rsc.li/rsc-advances

Introduction

The textile industrial dyestuffs create one of the primary sets of organic compounds that characterize an accumulative environmental hazard, while 1–20% of the total world production of dyes is used in the dyeing process and discharged as the textile effluent in running streams.[1] The extensive use of dyes is problematic due to the consumption of a vast quantity of water; only a small amount of the dyes is used in dye fabrication, while a large quantity is discarded into the environment, which causes pollution. The colored dye effluents are as such non-toxic, but they modify the ecosystem of the aquatic life in streams and other water bodies *via* reducing the underwater photosynthetic activity due to the unavailability of sunlight.[2] Even the lowest amount of a dye produces a color that is extremely visible in the effluent, thereby directly indicating that water has been polluted; also, removing the dye is challenging due to its complex chemical structure.[3,4] Different varieties of dyes such as acidic, basic, disperse, azo, diazo, anthraquinone-based, and metal complex dyes are used; these dyes are highly resistant to fading when exposed to light, water, and many chemicals.[5–7]

Department of Chemistry, University of Karachi, 75270, Karachi, Pakistan. E-mail: rafiasaeed200@yahoo.com

There are various methods available that are under practice for the treatment of industrial textile effluents after biological treatments to make them safe.[8,9] These processes include (i) Fenton (H_2O_2/Fe^{2+}), (ii) Fenton-like (H_2O_2/Fe^{3+}), (iii) photo-assisted Fenton ($H_2O_2/Fe^{2+}(Fe^{3+})$/UV and H_2O_2/Fe^{3+}-oxalate/UV), and (iv) ozonation (Mn^{2+}/oxalic acid/ozone and O_3/H_2O_2) reactions as well as (v) advanced oxidation process (AOP) (O_3/UV and H_2O_2/UV) and photocatalysis ($TiO_2/h\upsilon/O_2$).

The photo-Fenton process used for the degradation of Congo red (CR) utilizes Fe^{3+}/peroxy disulfate, Fe^0/H_2O_2/UV, and Fe^0/ammonium persulfate (APS)/UV, where 4-amino, 3-azo naphthalene sulphonic acid, quinol, dihydroxy-substituted naphthalene, dihydroxy-substituted biphenyl, hydroquinone, and phenol are formed as reaction intermediates. In the Fe^{3+}/peroxy disulfate system, degradation decreases with an increase in the concentration of the dye and pH. APS shows improved oxidation than H_2O_2 in treating the industrial effluent of the Congo red dye.[10,11]

The biogenic materials prepared by oyster shells show excellent properties related to the surface area including porosity, sorption capacity, and high concentration of $CaCO_3$, which can be characterized by FTIR, SEM, and BET techniques. The results show the excellent properties of AG25 in a dose-dependent manner.[12] Lin *et al.* (2018)[13] reported 100%

This journal is © The Royal Society of Chemistry 2019

Open Access Article. Published on 19 November 2019. Downloaded on 12/9/2025 3:22:16 AM.
This article is licensed under a Creative Commons Attribution-NonCommercial 3.0 Unported Licence.

removal of methylene green in 6 to 10 min using a heterojunction photocatalyst, namely, Ag_3PO_4@MWCNTs@Cr:$SrTiO_3$ under natural solar radiation and visible light irradiation.

The current practices of textile dye wastewater remediation and minimization are a severe threat due to the risk associated with its color to the running water streams. The usual management procedures involved in textile wastewaters are elimination by activated carbon adsorption, coagulation/flocculation, and membrane separation (ultrafiltration, reverse osmosis), but these processes are not the comprehensive solution of the removal of pollutants, while a biological treatment is not an exact solution due to the biological resistance of some dyes.[14–18] Thus, the dye wastewater management requires ultra-advanced processes for the recovery of colored water with the elimination of all relative byproducts by using the developed method. Therefore, for this purpose, the oxidizing agent $KMnO_4$ was used due to its preventive nature instead of any other compound of a high oxidative potential for the preservation of water bodies. Mn is an essential micronutrient for both plants and animals and can be easily removed/consumed by a marine organism. The aims and objectives of this innovation were to develop an ultra-advanced oxidation method for the recovery of thousands of tons of water discharged during dyeing and finishing processes with a lot of chemical additives used during dye fabrication. For this purpose, Congo red was selected, and the kinetics were monitored at various operational parameters for the establishment of the mechanism of dye degradation in the presence of all the dye fabricated additives. The application of current ACOP is discussed in the relative section of this article using real dye water samples with several other dyes.

Experimental

Materials and methods

Chemicals, materials, instruments and removal methods. The sodium salt of benzidinediazo-bis-1-naphthylamine-4-sulfonic acid referred to as Congo red (CR) belongs to the class azo and is used to dye cotton fabrics, as the acid-base indicator dye, and as a synthetic medicine dye. CR dye was purchased from the local dye dupatta center and used without any additional purification. The structure and chemical formula of CR are shown below in Fig. 1.

A stock solution of 0.001 M of CR was prepared using double distilled water and diluted according to the requirement of the experiment. A standard method was employed for the preparation of aqueous solutions of $KMnO_4$, acids, organic and inorganic additives and diluted according to the requirement of the experiment. During the experiment, the concentration of dye in the aqueous solution was determined by comparing the visible range spectrum with the standard solutions *via* a Shimadzu 1800 UV-Vis spectrophotometer. The wavelength maximum (λ_{max}) of CR was 497 nm.

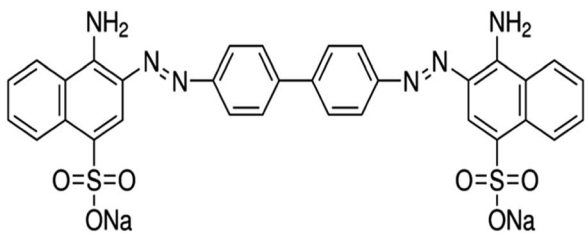

Fig. 1 The chemical structure of Congo red.

The percent de-coloration of CR was determined by using the following equation:

$$\text{Percentage of Decoloration} = \frac{A_o - A_t}{A_t} \quad (1)$$

HPLC analysis of the degraded dye product. The degraded product of CR was subjected to HPLC analysis for the validation of UV spectral analysis. The dye solution before and after the accomplishment of reaction was analyzed by the reversed-phase HPLC technique, where each sample was filtered through a 0.45 μm filter and then, 20 μL of the volume was loaded to HPLC, equipped with a C-18 column (250 mm × 4.6 mm). The mobile phase was prepared by using acetonitrile and water (HPLC grade) in a ratio of 65 : 35, followed by filtration through a 0.45 μm filter and degassed with the help of ultrasonic waves before use. The elution time of the Congo red dye was reported to be 2.9 min. The analysis was performed on the isocratic system, where the mobile phase was set at the flow rate of 1 mL min^{-1} and the absorbance was recorded at 495 and 278 nm through a deuterium lamp.[19]

Analytical analyses. The mineralization of CR was determined by chemical oxygen demand (COD) of the de-colorized filtrate by using the standard method stated in (APHA, 2005)[20] and COD analyzer APHA 5220 C. The COD values of both acidic filtrate and it's neutralized form were calculated and compared with the literature value of CR wastewater. The degraded product in the filtrate and residue after mineralization was identified by FTIR and compared with the dye and $KMnO_4$ peaks before and after oxidation. The salinity of the recovered water was determined through a Benchtop Conductivity/TDS meter, Model Jenway 4510, before and after the reaction.

Results and discussion. CR is a synthetic dye in which the π to π* and n to π transitions are responsible for its color. When these transitions were affected by an oxidant ($KMnO_4$), the color of the dye disappeared. It was observed that the reaction was valid in light as compared to that in dark, which was linked with the property of the oxidant ($KMnO_4$) that it is light-sensitive.

The kinetics of the reaction

The current investigation at various operational parameters described the newly developed advanced catalytic oxidation process (ACOP) for the oxidation of CR. The reaction was carried out at various concentrations of the dye (CR), oxidant ($KMnO_4$), pH, and temperature, and diverse organic (naphthalene and urea) and inorganic (NaCl and alum) additives. These additives are commonly employed for dye fixing for cellulose fibers. The rate of reaction at elevated concentrations of various additives proved that it is cost-effective. The current ACOP covers the following steps: (i) taking a dye solution and adding $KMnO_4$, (ii) activation of $KMnO_4$ by adding H_2SO_4, (iii) adding TiO_2 as

Open Access Article. Published on 19 November 2019. Downloaded on 12/9/2025 3:22:16 AM.
This article is licensed under a Creative Commons Attribution-NonCommercial 3.0 Unported Licence.

a catalyst for speeding up the oxidation reaction, (iv) additives and pH adjustment, (v) filtration and (vi) monitoring the optical density. The mole ratio between the dye and $KMnO_4$ was 1 : 1 without any difference in the concentration; this indicated that at a low concentration, the new ACOP was cost-efficient and eco-friendly. Permanganate-based advanced catalytic oxidation and the use of TiO_2 as a catalyst have been widely investigated and reported[1,18,22,23,26] in the literature, showing higher degradation efficiency; however, the current photocatalytic activity of permanganate-TiO_2/H^+-based oxidation that leads to complete mineralization has been found to be very effective in the presence of all dye additives and is thus used in dye fabrication in the absence of UV irradiation.

Effect of dye concentration on the oxidation of CR

The effect of the initial dye concentration of CR was monitored under new ACOP as a chief parameter in wastewater treatment with $KMnO_4$. The maximum de-coloration of CR was 98.59% at 1×10^{-4} M concentration of dye (Table 1), which was more than the values previously reported by Agustina and Ang (2012),[14] who reported 94.5% to 81% of color removal under the Fenton reaction for RB 4 and RR 2 at concentrations from 20 to 200 ppm, respectively, within 60 min from 100% to 91.5%. Vaigan *et al.* (2009)[15] reported that the de-coloration efficiency decreased from 57 to 31% in an SBR batch system for the concentration of Reactive Blue B-16 dye (20 to 40 mg L^{-1}, respectively). It was observed in the current investigation that % de-coloration was unaffected by the increase in the concentration of the dye, which clearly indicated that nascent oxygen (a reaction intermediate) was involved in dye degradation. It was a fractional order of 2/5 kinetics concerning the dye, while the spectral scan at each elevated concentration of the dye showed the formation of a complex of the dye with an oxidant, which later degraded into small fragments (Fig. 2).

Effect of oxidant concentration on the oxidation of CR

To make the current ACOP more effective and competitive with other existing processes of AOPs,[20–26] the effect of the incremental concentration of the oxidant $KMnO_4$ (5×10^{-4} and 7.5×10^{-4}) on the decoloration of the dye was investigated. It was fractional order kinetics, while de-coloration (Table 1) decreased (27.10% and 38.56%) at elevated concentrations (5×10^{-4} and 7.5×10^{-4}, respectively) as the excess of $KMnO_4$ left behind could be easily observed in the UV-Visible spectral scan through its peak in the visible region (Fig. 3). The objective of this estimation was to select the best operational dosage of $KMnO_4$ in ACOP. The current ACOP is more advantageous over any other reaction as [O] is released during the reaction, which is an important parameter; also, it is required as an electron scavenger to sustain the catalytic degradation reaction. The results of the current investigation were similar to the results reported by Chakrabarti and Dutta (2004),[17] who reported the requirement of a well-regulated air (oxygen) flow into the photocatalytic system as the reduced movement of oxygen can bring about an antagonistic effect on the photocatalytic reaction. The current results were also in accordance with those reported by

Table 1 Effect of various concentrations of dye, oxidant, acid, and catalyst on the decoloration of Congo red

[Conc.]	$k_0 = dx/dt$ (10^{-3}) mol dm^{-3} min^{-1}	k_1 (10^{-3}) min^{-1}	k_2 (10^{-2}) mol^{-1} dm^3 min^{-1}	R^2	% De-coloration
[Dye] (10^{-4}) mol dm^{-3}					
0.8	3.7	28.9	36.68	0.329	93.55
0.9	4.4	30.1	36.9	0.303	95.01
1.0	4.9	44.2	97.63	0.395	98.59
2.0	6.6	15.7	6.47	0.180	91.45
3.0	13.1	25.3	11.6	0.193	95.75
[Oxidant] (10^{-4}) mol dm^{-3}					
0.5	3.1	12.6	7.79	0.163	91.28
0.75	3.6	22.3	27.64	0.213	93.77
1.0	4.9	44.2	97.63	0.395	98.59
5.0	2.3	4.4	0.85	0.712	27.10
7.5	5.4	6.5	0.79	0.77	38.56
[H_2SO_4] mol dm^{-3}					
0.01	4.6	29.5	29.19	0.378	93.30
0.02	4.9	44.2	97.63	0.395	98.59
0.03	4.8	29.7	27.25	0.415	91.90
0.04	4.6	26.4	21.32	0.398	90.81
0.05	4.8	31.6	31.09	0.418	93.15
[TiO_2] g/50 mL					
0.05	4.5	28.9	29.37	0.355	92.06
0.075	4.6	27.7	24.64	0.378	87.54
0.1	4.9	44.2	97.63	0.395	98.59
0.25	4.8	35.9	45.1	0.387	95.16
0.5	4.9	35.8	42.55	0.403	94.55

Open Access Article. Published on 19 November 2019. Downloaded on 12/9/2025 3:22:16 AM.
This article is licensed under a Creative Commons Attribution-NonCommercial 3.0 Unported Licence.

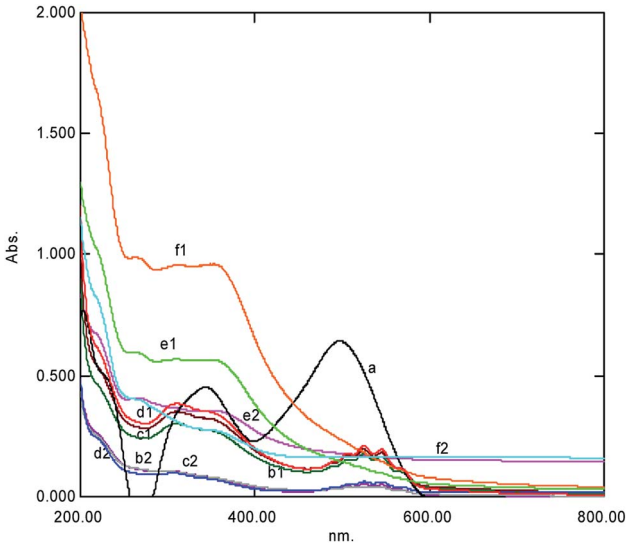

Fig. 2 The UV-Visible spectral change at various concentrations of Congo red after 5 min showing complex formation represented by (1) degradation (2) observed within one hour simultaneously (a = Dye, b = 8×10^{-5} M, c = $9 \times 1\,0^{-5}$ M, d = 1.0×10^{-4} M, e = 2.0×10^{-4} M, and f = 3.0×10^{-4} M).

Saquib *et al.* (2008);[18] they observed the decoloration of Patent Blue VF (2) and Fast Green FCF (1) in the presence of hydrogen peroxide (H_2O_2), ammonium persulphate ($(NH_4)_2S_2O_8$), and potassium bromate using Hombikat UV 100 and found that it is useful in the degradation of both dyes.

Effect of acid concentration on the oxidation of CR

The rate of oxidation monitored in the presence of hydrochloric acid (HCl) and sulphuric acid (H_2SO_4) showed no de-coloration in the presence of HCl. Therefore, H_2SO_4 was used as a medium

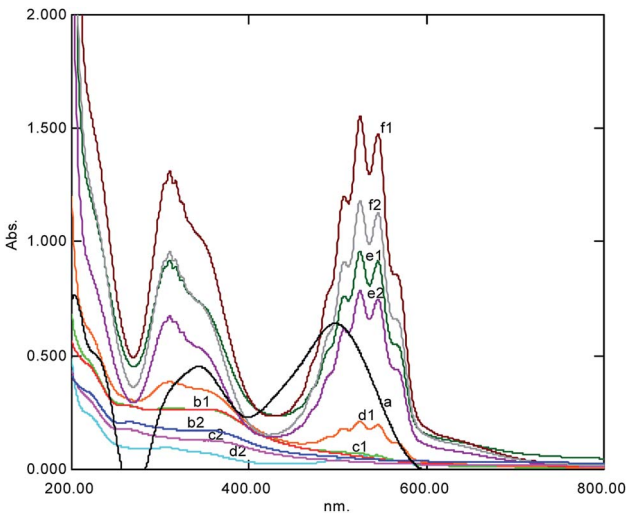

Fig. 3 The UV-Visible spectral change at various concentrations of $KMnO_4$ after 5 min showing complex formation represented by (1) degradation (2) observed within one hour simultaneously (a = dye, b = 5×10^{-5} M, c = 7.5×10^{-5} M, d = 1×10^{-4} M, e = 5×10^{-4} M, and f = 7.5×10^{-4} M).

throughout the experiments, where zero-order kinetics was observed (Table 1). Moreover, no reaction with HCl indicated that not only protons but also sulfates were effective in the discoloration reaction. Also, chloride ions reacted with manganese to give $MnCl_2$, which deactivated the manganese ions according to the following equation:

$$2KMnO_4 + 16HCl \rightarrow 2KCl + 2MnCl_2 + 8H_2O + 5Cl_2 \quad (2)$$

$$MnCl_2 + \text{Dye} \rightarrow \text{no reaction} \quad (3)$$

H_2SO_4 in combination with $KMnO_4$ releases [O], which was found to be effective in de-coloration according to the following reaction steps:

$$2KMnO_4 + 3H_2SO_4 \rightarrow K_2SO_4 + 2MnSO_4 + 3H_2O + 5[O] \quad (4)$$

$$\text{Dye} + [O] \rightarrow \text{degraded product} \quad (5)$$

The role of sulphates cannot be roled out in the presence of a catalyst according to the following equation:

$$SO_4^{2-} + e_{CB}^{-} \rightarrow SO_4^{-\bullet} \quad (6)$$

$$SO_4^{-\bullet} + H_2O \rightarrow SO_4 + H^+ + O \quad (7)$$

Usually, an advanced oxidation process, including the Fenton reaction, is a highly pH-reliant process due to the role of OH production, which is formed in acidic conditions.[4,6] Therefore, the current ACOP was investigated for the maximum degradation at various pH values in the range of 2–9 using either H_2SO_4 or NaOH. It was found that lower pH was more effective and [O] was the main oxidant in the acidic medium. Lachheb *et al.* (2002)[21] reported that a pH value below 6 was found to be suitable for the degradation of CR or azo dyes in the presence of TiO_2, where strong adsorption of azo dyes was observed as a consequence of the electrostatic attraction of the positively charged TiO_2 with the dye; this was similar to the results reported by Rupa *et al.* in 2007.[22] The current results showed that the alkaline medium was not effective as the dye molecules were negatively charged, which decreased the adsorption capability, while they were adsorbed more readily on the TiO_2 particles in the acidic medium. At elevated concentrations of $KMnO_4$, excess oxidant was left behind, which can be easily observed by its peak in the visible region of the UV-Visible spectral scan (Fig. 4). The final pH at the end of the reaction was found through a pH meter; it was acidic but was maintained neutral by the addition of a small amount of alkali.

Effect of catalyst concentration on the oxidation of CR

TiO_2, having an essential damaging nature, which may lead to the complete mineralization of organic carbon into CO_2, was used here to accelerate the reaction as a catalyst because the reaction was prolonged and required almost 48 h for completion. The addition of TiO_2 reduced the time interval and 98% de-coloration was achieved in 1 h (Table 1, Fig. 5). The mechanism involved in the Ti-mediated AOP suggested that the dye adsorbed on the catalyst surface, where e^- from Mn and the

Open Access Article. Published on 19 November 2019. Downloaded on 12/9/2025 3:22:16 AM.
This article is licensed under a Creative Commons Attribution-NonCommercial 3.0 Unported Licence.

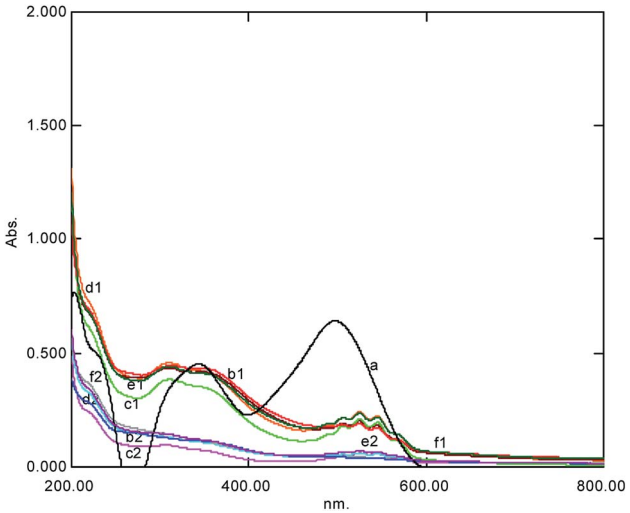

Fig. 4 The UV-Visible spectral change at various concentrations of H_2SO_4 after 5 min showing complex formation represented by (1) degradation (2) observed within one hour simultaneously (a = dye, b = 0.01 M, c = 0.02 M, d = 0.03 M, e = 0.04 M, and f = 0.05 M).

catalyst coupled with oxygen, played an effective part in degradation. The % degradation of CR was found to be approximately the same, with an increase in the concentration of the catalyst (0.05 to 2.5 g/50 mL); this was comparable with the results by Rupa *et al.* (2007)[22], who reported 80% de-coloration at the concentrations from 1.5 to 3.00 g L^{-1}. The % de-coloration with time suggests that an increase in the catalyst quantity does not affect the % de-coloration with time (Fig. 5). The possible acceleration in the reaction in the presence of the catalyst[1] occurred according to the following reaction pathway:

$$2KMnO_4 + 3H_2SO_4 \rightarrow K_2SO_4 + 2MnSO_4 + 3H_2O + 5[O] \quad (8)$$

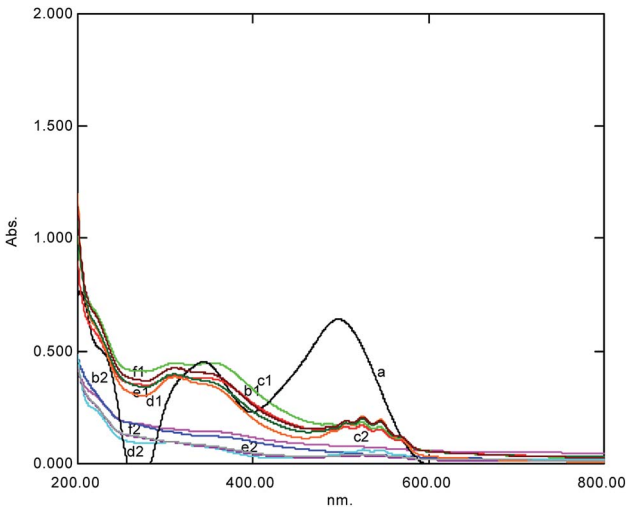

Fig. 5 The UV-Visible spectral change at various amounts of TiO_2 after 5 min showing complex formation represented by (1) the degradation (2) observed within one hour simultaneously (a = dye, b = 0.05 g/50 mL, c = 0.075 g/50 mL, d = 0.1 g/50 mL, e = 0.25 g/50 mL, and f = 0.5 g/50 mL).

$$\text{Dye} + h\upsilon\ (\text{Vis}) \rightarrow {}^1\text{Dye}^* \text{ or } {}^3\text{Dye}^* \quad (9)$$

$${}^1\text{Dye}^* \text{ or } {}^3\text{Dye}^* + 5[O] \rightarrow \text{degradation product} \quad (10)$$

$${}^1\text{Dye}^* \text{ or } {}^3\text{Dye}^* + TiO_2 \rightarrow \text{Dye}^+ + TiO_2\ (e_{CB}^-) \quad (11)$$

$$\text{Dye}^+ \rightarrow \text{degradation product} \quad (12)$$

The effect of a change in temperature

The effect of a change in temperature showed that the reaction was independent of temperature. In contrast, a detailed literature search showed that temperature plays a vital role. Xu *et al.* (2005)[23] reported that in the batch experiment, potassium permanganate was effective for the decolorization of 10 types of dyes at various concentrations and elevated temperatures, while Benetoli *et al.* (2011)[24] showed that the effect of temperature on the decolorization of methylene blue (MB) increased with a rise in temperature in the range from 4 to 28 °C; no effect of temperature in the range from 28 to 37 °C was observed with the activation energy being 13.09 kJ mol^{-1}, which was found to be higher than the energy of activation of current ACOP (E_a = 0.9495 kJ mol^{-1}). Medien and Khalil (2010)[25] reported that the rise in temperature increases the rate of oxidation of crystal violet (CV), Malachite green (MG), Rhodamine B (RB), and methylene blue (MB) under Fenton oxidation. Moreover, the energy of activation showed the high efficiency of the reaction. The thermodynamic activation parameters (Table 2) showed that E_a decreased with an increase in the temperature, which was effective for the activation of the oxidant in the acidic medium. The values of enthalpy of activation (ΔH), free energy of activation (ΔG), and entropy of activation (ΔS) showed that no solvated states were present in the reaction mixture,[26–29] and CR degradation occurred through the complex formation with the oxidant $KMnO_4$. The current investigation proves that new ACOP is cost-effective as no extra energy is required for the acceleration of the rate of reaction.

Effect of dye additives

Urea and naphthalene are famous in the dye industry as dye fixers on fabrics and are released as additives in water bodies with dye wastewater, which makes the dye wastewater more complex and challenging to treat. Therefore, these two additives were considered in the current new AOP system. The effects of

Table 2 Thermodynamic activation parameters for Congo red oxidation

Temperature K	E_a kJ mol^{-1}	ΔG kJ	ΔH kJ mol^{-1}	ΔS kJ K^{-1} mol^{-1}
288	0.9495	12.786	−1.445	−0.049
298		12.933	−1.528	−0.049
308		13.623	−1.611	−0.05
318		13.907	−1.694	−0.049
328		14.344	−1.778	−0.049

 This journal is © The Royal Society of Chemistry 2019

Open Access Article. Published on 19 November 2019. Downloaded on 12/9/2025 3:22:16 AM.
This article is licensed under a Creative Commons Attribution-NonCommercial 3.0 Unported Licence.

Table 3 Effect of concentration of organic and inorganic additives on de-coloration of dye with $KMnO_4$ (Congo red = 1×10^{-4} M, $KMnO_4 = 1 \times 10^{-4}$ M, H_2SO_4 = 0.02 M, TiO_2 = 0.1 g/50 mL, temperature = 298 K)

[Conc.] mol dm^{-3}	$k_0 = dx/dt$ (10^{-3}) mol dm^{-3} min^{-1}	k_1 (10^{-3}) min^{-1}	k_2 mol^{-1} dm^3 min^{-1}	R^2	% De-coloration
Urea					
0.001	4.9	56.2	1.7073	0.362	98.29
0.005	5.1	41.6	0.6075	0.417	96.26
0.01	5	38.5	0.507	0.409	95.33
0.05	5.1	40.9	0.5758	0.409	95.48
0.1	4.7	28.2	0.2492	0.386	91.12
Naphthalene					
0.001	4.9	31.6	0.3146	0.403	93.15
0.005	4.9	36.6	0.444	0.407	94.24
0.01	5	36.4	0.4265	0.416	93.93
0.05	4.9	30.4	0.2781	0.427	92.99
0.1	4.7	29.8	0.2781	0.397	92.37
Potash alum					
0.001	3.8	31.7	0.6474	0.217	96.73
0.005	3.5	26.4	0.4916	0.194	96.42
0.01	3.7	68.8	10.043	0.198	100
0.05	4	47.2	1.9751	0.24	99.22
0.1	3.9	42.9	1.4465	0.230	98.44
Sodium chloride					
0.001	5	48.6	0.9919	0.387	97.35
0.005	5.2	86.8	3.6748	0.396	100
0.01	5.2	83.9	5.829	0.406	100
0.05	5.2	98.2	6.511	0.383	100
0.1	5.2	86.1	6.1992	0.396	100

the added organic additives, *i.e.*, urea and naphthalene were investigated, and it was found that the rate of reaction was independent of the added organic additives (Table 3). Moreover, it was established that present AOP was advantageous in the degradation of dye wastewater in the presence of these critical dye additives.[28] Similarly, we added inorganic additives, such as NaCl and alum, which are also used in various dye processes, and they were also investigated under developed AOP. It was found that new AOP was also valuable in the treatment of the complex nature of the dye wastewater (Fig. 6) and the dye wastewater could be restored completely in the presence of dye additives.

Furthermore, literature[30] search showed the oxidative degradation of Blue 2B (B54) and Red 12B (R31) by the Fenton's reagent in an aqueous medium with two added inorganic ions like Cl^- and SO_4^{-2}. Hu *et al.* (2003)[30] reported the effect of various ions on dyes like azo dyes, Procion Red MX-5B (MX-5B), and Cationic Blue X-GRL (CBX) in the presence of UV-illuminated TiO_2 and showed that the rate of decolorization was enhanced due to irradiation. They also reported that the reaction was useful for the treatment of dye wastewater. The plot of % de-coloration with respect to time in the treatment of dye wastewater showed that it was found operational in the treatment of CR in the presence of various kinds of additives (Fig. 7).

Mineralization of CR

The mineralization of the dye was studied in relation to the released oxygen as the main oxidant and CO_2 as the main degraded product of CR. Therefore, the reaction mixture was prepared in a round bottom flask, and we tried to collect the gas in a water-filled gas jar placed in a water bath. No displacement of water into the gas jar showed that oxygen was not released, thereby suggesting that oxygen was used in the degradation of

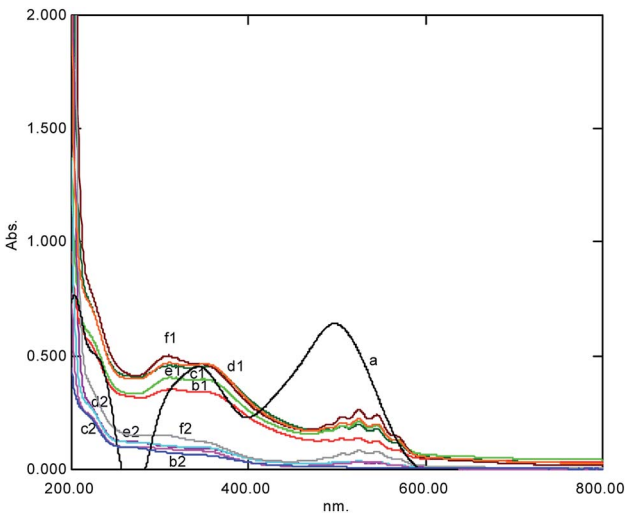

Fig. 6 The UV-Visible spectral change at various concentrations of urea after 5 min showing complex formation represented by (1) the degradation (2) observed within one hour simultaneously (a = dye, b = 0.001 M, c = 0.005 M, d = 0.01 M, e = 0.05 M, and f = 0.1 M).

Open Access Article. Published on 19 November 2019. Downloaded on 12/9/2025 3:22:16 AM.
This article is licensed under a Creative Commons Attribution-NonCommercial 3.0 Unported Licence.

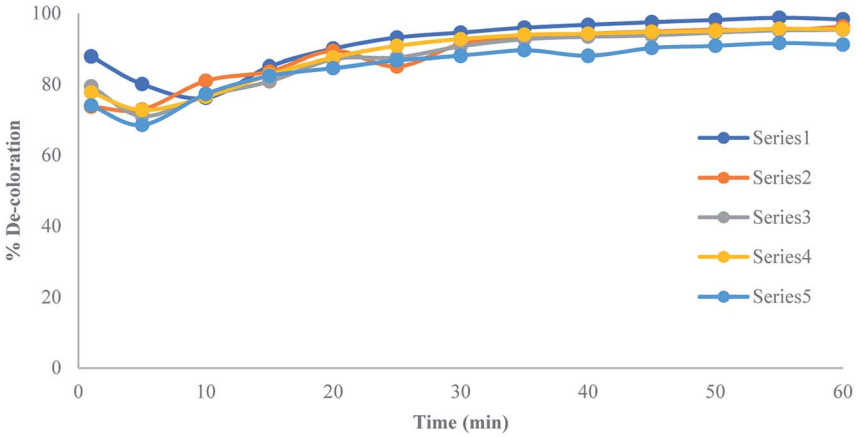

Fig. 7 A plot of % de-coloration and time in the presence of diverse ions.

the dye. The mineralization of the dye into CO_2 was tested through limewater, where the formation of a white precipitate of $CaCO_3$ showed that the dye finally degraded into CO_2 and H_2O. This test showed that CO_2 gas was produced during the reaction, but no traces of the O_2 gas in the reaction proved that it was utilized in oxidation. The reaction was also carried out in the absence of O_2 by seal packing the reaction vessel, and it was found that the oxidation of the dye occurred due to the evolution of an [O] radical, which oxidized the double bond of C=C and converted it into CO_2 through the degradation of the organic compound CR. The test for COD showed that it decreased from 3000 ppm to 71.2 ppm by this method, whereas by neutralizing the filtrate, it was reduced to 53.6 ppm.[31] The OH radical formation was also tested *via* benzoic acid. No effervescence on the addition of benzoic acid showed that OH radicals were not the part of current ACOP and degradation occurred *via* the released oxygen according to the following equation:[26]

$$2KMnO_4 + 3H_2SO_4 \rightarrow K_2SO_4 + 2MnSO_4 + 3H_2O + 5[O] \quad (13)$$

The complete color removal of the dye (Fig. 3) initiated the change in the oxidation state of Mn from Mn^{7+} to Mn^{2+}:

$$\underset{\text{Colored}}{Mn^{7+}} + 5e^- \rightarrow \underset{\text{Colorless}}{Mn^{2+}}$$

FTIR studies of ACOP

The FTIR spectra of the dye before de-coloration in an aqueous medium are presented in Fig. 8a and compared with the FTIR spectrum of the reaction mixture of the dye and $KMnO_4$ after de-coloration (Fig. 8b and c). The observed FTIR spectral peak of the CR dye (Fig. 8a) showed stretching of N–H at 34 622.22 and 2370.51 cm^{-1} as in charged amines (C=NH–), and the peak at 1649.14 cm^{-1} corresponded to the double bond stretching of –N=N– as in an azo compound (Table 4). The specific peaks at 1390.68, 1193.94, and 1112.93 cm^{-1} were attributed to the C=C stretching of an aromatic compound, S=O stretching, and C–N vibration of aliphatic amines, respectively. The peaks at 746.45 and 617.22 cm^{-1} were due to the CH deformation of the benzene ring.[31] The spectrum of the decolorized filtrate (Fig. 8b) indicates that the three peaks ascribed to water at 3406.29, 1637.56, and 2083.12 cm^{-1} are due to the O–H stretching of H-bonding, scissor bending of O–H–O, and coupled peak of scissor bending and broadband, respectively (Table 4). Also, the peaks at 597.93, 1107.14, 1384.89, and 2362.8 cm^{-1} were attributed to the =C–H bending of an alkene, C–N stretching of amine, S=O bending, and –C=C– stretching, respectively.[32] This indicated that the decolorization of CR was linked to the breaking of azo bonds, which was related to the breaking of chromophores, *i.e.*, unsaturated conjugated bonds, namely, –N=N– in the dye,[32] where the entire de-aromatization of the dye was related to the current ACOP process.

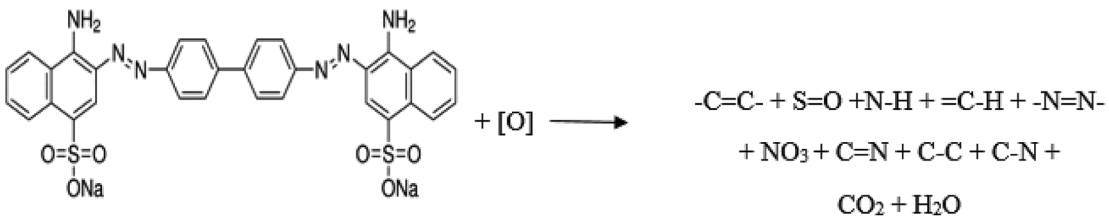

Open Access Article. Published on 19 November 2019. Downloaded on 12/9/2025 3:22:16 AM.
This article is licensed under a Creative Commons Attribution-NonCommercial 3.0 Unported Licence.

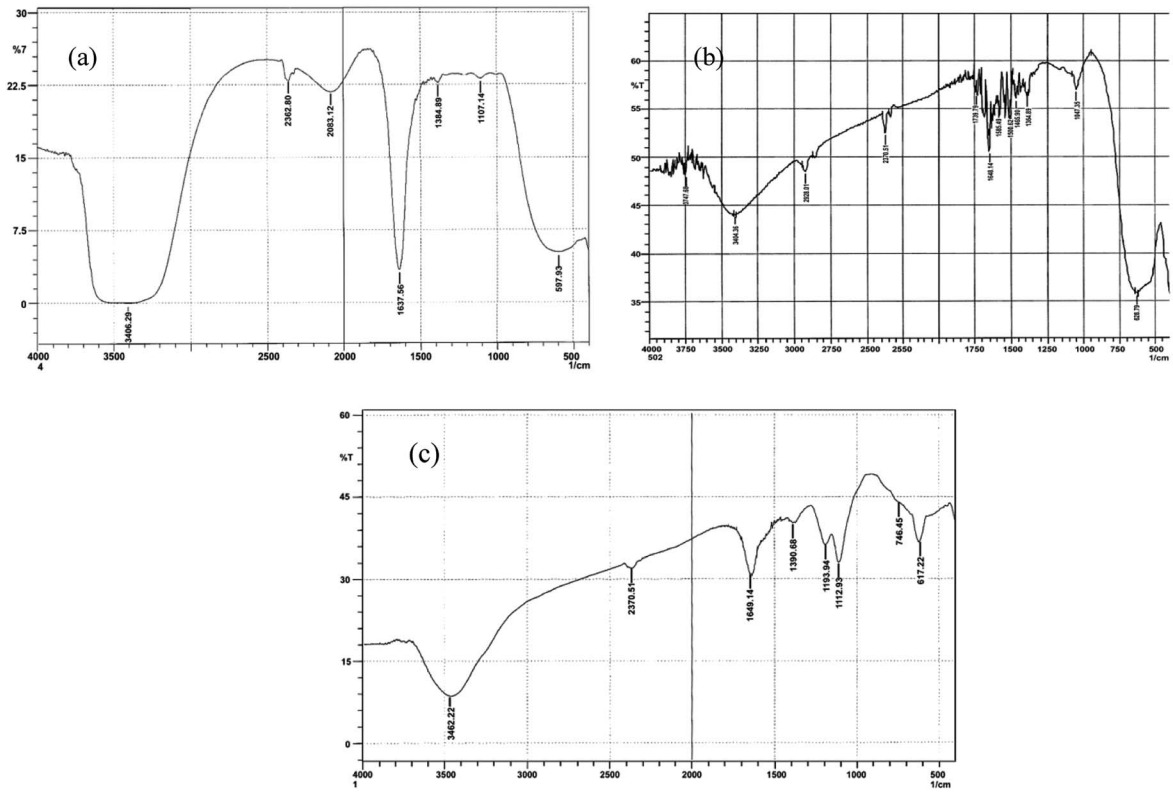

Fig. 8 (a) The infrared spectrum of Congo red; (b) the FTIR spectrum of the decolorized form of dye; (c) the FTIR spectrum of sludge formed after dye mineralization.

Table 4 Dye peaks in the de-colorized filtrate and sludge

Dye peaks	De-colorized filtrate	Sludge
N–H	Absent	Present
N═N	Absent	Present
C═C	Present	Absent
S═O	Present	Absent
C–N	Present	Present
═C–H	Present	Present

Also, the sludge formed at the end of the reaction was subjected to FTIR, and the resulting spectrum (Fig. 8c) showed multiple peaks. The peaks at 3404.36 and 3747.69 cm^{-1} were due to the N–H stretching, while the peak at 1585.49 cm^{-1} was due to the bending of the N–H bond (Table 4). Furthermore, the specific peak at 2926.01 cm^{-1} was due to the stretching of the ═C–H bond, while there was another peak at a lower wavelength of 628.79 cm^{-1}, which appeared because of the bending of ═C–H of the alkene. The peaks at 1649.14 and 1739.79 cm^{-1} were attributed to –N═N– double bond stretching; the two bands at 1500.62 and 1384.89 cm^{-1} corresponded to the stretching of the nitro compound. Moreover, the peaks at 2370.51, 1465.90, and 1047.35 cm^{-1} were due to C═N stretching, bending of alkane, and C–N stretching of amine, respectively.[32]

HPLC analysis of the final product

The HPLC analysis of the final degraded product of the CR dye solution was performed, which proved the complete mineralization of the dye. Initially, the chromatograms of both the samples were established at 495 nm based on the reports of Choi and co-workers (2013).[19] The absorbance at the retention time of 1.749 min was recorded for the CR dye, where 100% concentration of the dye was eluted; however, the solution after treatment showed no absorbance at the same retention time (Fig. 9a and b). Furthermore, the dye solution before and after the reaction was scanned once again at a new absorbance of 278 nm. This wavelength was selected in the ultraviolet region because of the resultant solution, which became colorless after the treatment (Fig. 10a and b). The chromatograms recorded at 278 nm for the Congo red dye show two peaks at the elution times of 1.680 and 3.078 min (Fig. 10a), whereas the sample of Congo red after the treatment showed four disintegrated products at 1.448, 2.306, 3.360, and 3.760 min rather than at 3.077 min (Fig. 10b). It is clearly indicated in the chromatogram (Fig. 10b) that the characteristic peak of the Congo red dye at a retention time of 1.680 min in the ultraviolet region shifts to 2.306 min. In contrast, the five different eluted peaks shown in Fig. 10b indicate that the Congo red dye fragmented into other components.

Salinity of the recovered water. The salinity of the recovered water related to the mineralization of the dye wastewater through current new ACOP was tested for its possible reuse and

Open Access Article. Published on 19 November 2019. Downloaded on 12/9/2025 3:22:16 AM.
This article is licensed under a Creative Commons Attribution-NonCommercial 3.0 Unported Licence.

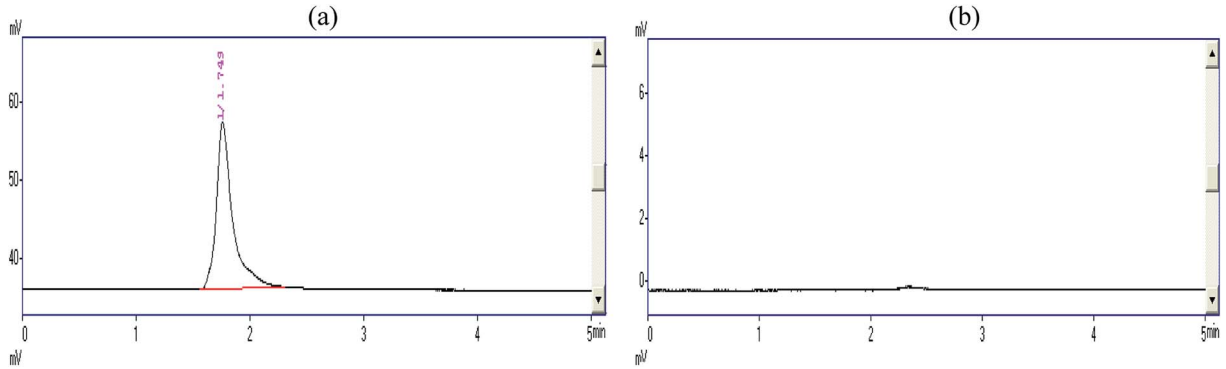

Fig. 9 (a) The HPLC chromatogram of Congo red dye and the absorbance spectrum recorded at 495 nm. (b) The HPLC chromatogram of solution resulting after the treatment and the absorbance spectrum recorded at 495 nm.

appropriate management. For this purpose, two commonly used methods, namely, the measurements of electrical conductivity (EC) and total dissolved solids (TDS) were employed. EC and TDS were monitored at the optimized concentrations of the dye, $KMnO_4$, H_2SO_4, and TiO_2, *i.e.*, 1×10^{-4} M, 1×10^{-4} M, 0.02 M, and 0.1 g/50 mL, respectively. The values of electrical conductivity and total dissolved solids increased (Table 5); this confirmed the mineralization of the dye into smaller fragments, due to which the electrical conductivity of the solution increased, followed by an increase in TDS coupled with an improvement in BOD/COD of the recovered water. The salinity and TDS of the recovered water were comparable with the salinity levels tolerable for livestock and other purposes (5970–7460 μS cm^{-1} or 5.9–7.5 dS m; 4000–5000 (mg L^{-1} or ppm)),[33] which proved that the new ACOP is eco-friendly, cost-effective, and easily manageable.

Application of current ACOP in real and several dye wastewater samples. After the successful development of current ACOP on CR dye wastewater restoration at the laboratory scale, it was applied to several dyes, including Reactive blue, Reactive yellow, acridine orange, methylene blue, and thionine, followed by real red dye wastewater, which was collected from a dye shop

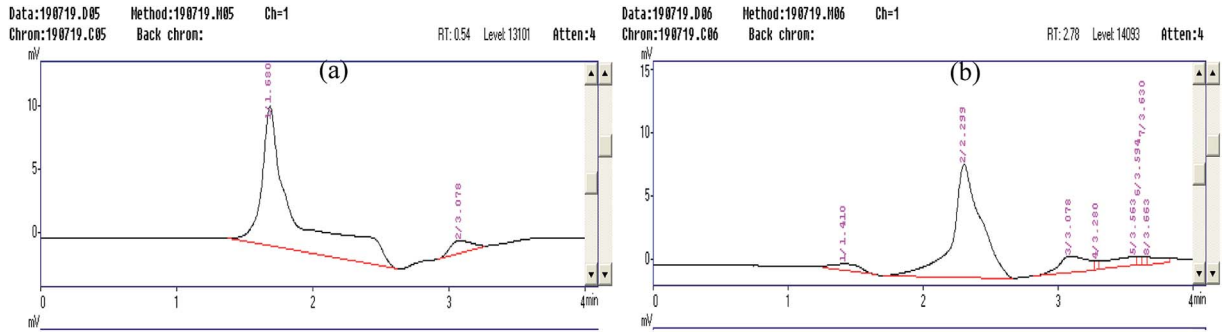

Fig. 10 (a) The HPLC chromatogram of Congo red dye and the absorbance spectrum recorded at 278 nm. (b) The HPLC chromatogram of solution resulting after treatment and the absorbance spectrum recorded at 278 nm.

Table 5 EC and TDS of the reaction[a]

Dye solution	Conductivity μS	TDS mg L^{-1}	Literature value[33]
Original dye solution	106.6	63.6	5970–7460 (μS cm^{-1}) or 5.9–7.5 (dS m^{-1}) 4000–5000 (mg L^{-1} or ppm)
After adding $KMnO_4$	125.4	75.3	
After adding H_2SO_4	126.3	75.9	
After adding TiO_2	127.3	76.4	
After complete de-coloration	5660	3390	
With all additives	5780	4000	

[a] Congo red = 1×10^{-4} M, $KMnO_4 = 1 \times 10^{-4}$ M, $H_2SO_4 = 0.02$ M, $TiO_2 = 0.1$ g/50 mL, temperature = 298 K, and distilled water conductivity = 18.31 μS.

Open Access Article. Published on 19 November 2019. Downloaded on 12/9/2025 3:22:16 AM.
This article is licensed under a Creative Commons Attribution-NonCommercial 3.0 Unported Licence.

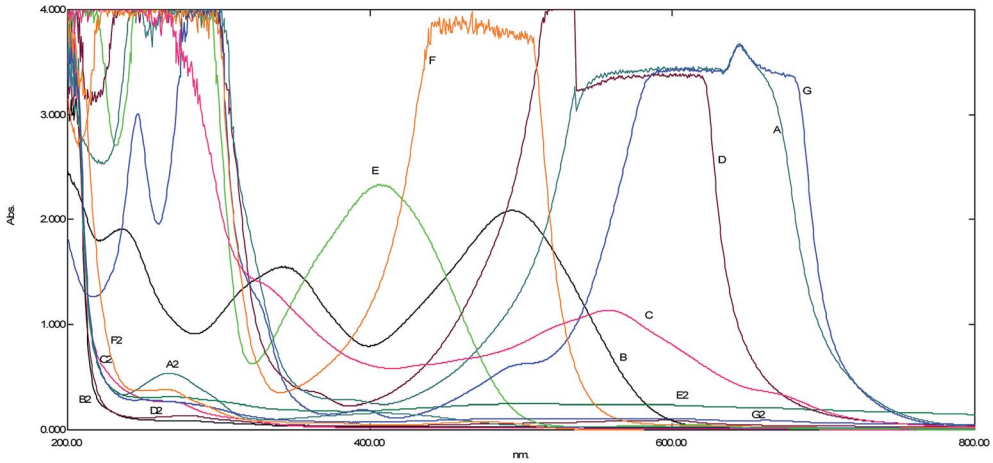

Fig. 11 The UV-Visible spectra showing the absorption peaks of different dyes: (A) dye wastewater, (B) Reactive red, (C) Reactive blue, (D) thionine, (E) Reactive yellow, (F) acridine orange, and (G) methylene blue. In contrast, the degradated product observed within one hour is represented by (2).

after its prime use of fabric dyeing. The observed spectral change after the application of ACOP on several dyes showed the complete mineralization of the colored wastewater with all the dye additives being used in dye fixing (Fig. 11). This showed that thousands of tons of dye wastewater could be restored for its reuse in the dye fabrication industry.

Conclusion

The new advanced catalytic oxidation process indicates its promising result for the decoloration and treatment of dye wastewater in the presence of organic and inorganic additives, which help the dye to fix onto the fabric and make the nature of the wastewater complex and challenging to treat. The decoloration of the dye with an oxidant ($KMnO_4$) was found to go through a complex formation step in the beginning, the complex later on undergo to the degradation with an increase in the salinity of the recovered water. This led to the conclusion that TiO_2 reduced the time interval, thereby providing 98.59% de-coloration within 1 h. It was also concluded that new ACOP was effective due to the generation of nascent oxygen [O] and e^- from the oxidant ($KMnO_4$) and catalyst (TiO_2). The dye peak shifted toward the region of shorter wavelength and higher region, indicating the formation of smaller dye fragments consisting of compounds having C=C, C–N, S=O, or =C–C bonds, which was confirmed through FTIR and HPLC; these compounds were later converted to CO_2. The sludge formed at the end of the degradation reaction was subjected to FTIR, which showed the formation of the smaller degraded products of functional groups N–H, =C–H, C=N, and N=N.

Conflicts of interest

It confirmed that there is no conflict of interest in between authors.

Acknowledgements

The author is very thankful to HEC Pakistan for providing financial support through Research Project No. 20-2282/NRPU/R&D/HEC/12/5014.

References

1 I. K. Konstantinou and T. A. Albanis, *Appl. Catal., B*, 2004, **49**, 1–4.
2 G. E. Walsh, L. H. Bahner and W. B. Horning, *Environ. Pollut. Ecol. Biol.*, 1980, **21**, 169–179.
3 P. Nigam, G. Armour, I. M. Banat, D. Singh and R. Marchant, *Bioresour. Technol.*, 2000, **72**, 219–226.
4 K. C. Chen, J. Y. Wu, D. J. Liou and S. C. Hwang, *J. Biotechnol.*, 2003, **101**, 57–68.
5 V. J. Poots, G. McKay and J. J. Healy, *Water Res.*, 1976, **10**, 1061–1066.
6 V. J. Poots, G. McKay and J. J. Healy, *Water Res.*, 1976, **10**, 1067–1070.
7 G. McKay, *Am. Dyest. Rep.*, 1979, **68**, 29.
8 A. Altaf, S. Noor, Q. M. Sharif and M. Najeebullah, *J. Chem. Soc. Pak.*, 2010, **32**, 115–116.
9 R. Andreozzi, V. Caprio, A. Insola and R. Marotta, *Catal. Today*, 1999, **53**, 51–59.
10 L. G. Devi, S. G. Kumar and K. M. Reddy, *Cent. Eur. J. Chem.*, 2009, **7**, 468–477.
11 L. Gomathi Devi, S. Girish Kumar, K. Mohan Reddy and C. Munikrishnappa, *Desalin. Water Treat.*, 2009, **4**, 294–305.
12 X. Inthapanya, S. Wu, Z. Han, G. Zeng, M. Wu and C. Yang, *Environ. Sci. Pollut. Res.*, 2019, **26**, 5944–5954.
13 Y. Lin, S. Wu, X. Li, X. Wu, C. Yang, G. Zeng, Y. Peng, Q. Zhou and L. Lu, *Appl. Catal., B*, 2018, **227**, 557–570.
14 T. Agustina and H. Ang, *Int. J.*, 2012, **3**, 141–148.
15 A. Vaigan, M. A. Moghaddam and H. Hashemi, *J. Environ. Health Sci. Eng.*, 2009, **6**, 11–16.

Open Access Article. Published on 19 November 2019. Downloaded on 12/9/2025 3:22:16 AM.
This article is licensed under a Creative Commons Attribution-NonCommercial 3.0 Unported Licence.

16 R. Azmat, N. Qamar, R. Naz and A. Khursheed, *Pak. J. Pharm. Sci.*, 2016, 29.
17 S. Chakrabarti and B. K. Dutta, *J. Hazard. Mater.*, 2004, **112**, 269–278.
18 M. Saquib, M. A. Tariq, M. Faisal and M. Muneer, *Desalination*, 2008, **219**, 301–311.
19 Y. S. Choi, Y. Long, M. J. Kim, J. J. Kim and G. H. Kim, *J. Environ. Sci. Health, Part A: Toxic/Hazard. Subst. Environ. Eng.*, 2013, **48**, 501–508.
20 American Public Health Association, APHA, *Standard Methods for the Examination of Water and Wastewater*, American Public Health Association, Washington DC, 21st edn, 2005, p. 1220.
21 H. Lachheb, E. Puzenat, A. Houas, M. Ksibi, E. Elaloui, C. Guillard and J. M. Herrmann, *Appl. Catal., B*, 2002, **39**, 75–90.
22 A. V. Rupa, D. Manikandan, D. Divakar, S. Revathi, M. E. Preethi, K. Shanthi and T. Sivakumar, *Indian J. Chem. Technol.*, 2007, **14**, 71.
23 X. R. Xu, H. B. Li, W. H. Wang and J. D. Gu, *Chemosphere*, 2005, **59**, 893–898.
24 L. O. Benetoli, B. M. Cadorin, C. D. Postiglione, I. G. Souza and N. A. Debacher, *J. Braz. Chem. Soc.*, 2011, **22**, 1669–1678.
25 H. A. Medien and S. M. Khalil, *J. King Saud Univ., Sci.*, 2010, **22**, 147–153.
26 R. Azmat, F. V. Mohammed and T. Ahmed, *Front. Chem. China*, 2011, **6**, 84.
27 R. P. Sontakke, A. K. Mishra and K. S. Muralidhara, *Study on physiochemical analysis of textile industry effluent and in vitro study of decolourization of the Congo Red acidic dye by bacterial species*, *Textile Value Chain*, 2016, https://textilevaluechain.in/2019/05/27/2326/.
28 R. Azmat, B. Yasmeen and F. Uddin, *Asian J. Chem.*, 2007, **19**, 1115.
29 P. K. Malik and S. K. Saha, *Sep. Purif. Technol.*, 2003, **31**, 241–250.
30 C. Hu, C. Y. Jimmy, Z. Hao and P. K. Wong, *Appl. Catal., B*, 2003, **46**, 35–47.
31 H. Lade, S. Govindwar and D. Paul, *Int. J. Environ. Res. Public Health*, 2015, **12**, 6894–6918.
32 B. L. Mojet, S. D. Ebbesen and L. Lefferts, *Chem. Soc. Rev.*, 2010, **39**, 4643–4655.
33 *Australian soil fertility manual*, ed. G. Price, CSIRO PUBLISHING, 2006.

 This journal is © The Royal Society of Chemistry 2019